Eur Biophys J (2004) 33: 633–643
DOI 10.1007/s00249-004-0405-4

ARTICLE

Arthur Vermeulen · Jean-Pierre Rospars

Why are insect olfactory receptor neurons grouped into sensilla? The teachings of a model investigating the effects of the electrical interaction between neurons on the transepithelial potential and the neuronal transmembrane potential

Received: 15 December 2003 / Revised: 10 March 2004 / Accepted: 19 March 2004 / Published online: 12 May 2004

Abstract Insect olfactory receptor neurons are compartmentalized in sensilla. In a sensillum, typically two receptor neurons are in close contact and can influence each other through electrical interaction during stimulation. This interaction is passive, non-synaptic and a consequence of the electrical structure of the sensillum. It is analysed in a sensillum model and its effects on the neuron receptor potentials are investigated. The neurons in a sensillum can be both sensitive to a given odorant compound with the same sensory threshold or with different thresholds, or only one neuron be sensitive to the odorant. These three types of sensilla are compared with respect to maximum amplitude, threshold and dynamic range of the potentials. It is found that gathering neurons in the same sensillum is disadvantageous if they are identical, but can be advantageous if their thresholds differ. Application of these results to actual recordings from pheromone and food-odour olfactory sensilla is discussed.

Keywords Intensity coding · Neuron modelling · Olfactory receptor neuron · Receptor potential · Sensillum

Introduction

Understanding how olfactory receptor neurons (ORNs) encode intensive, qualitative, temporal and spatial information about odour stimuli is an intriguing topic which has attracted much attention in recent years (Buck 1996; Hildebrand and Shepherd 1997; Krieger and Breer 1999). Building on our previous modelling work on these neurons (Rospars et al. 1996; Vermeulen and Rospars 1998a, 2001a, 2001b), we investigate here a neglected physiological aspect of olfactory transduction, the passive (non-synaptic) electrical interaction that takes place between two or more ORNs in close contact. In a favourable case, the insect olfactory system, we show that this interaction can modify the receptor potential of the neurons and consequently their information coding properties.

In insects, an olfactory sensillum consists of (usually) one to five ORNs, three auxiliary cells and an often hair-like cuticular formation (Fig. 1). These sensilla are located at the surface of the body, essentially on two head appendages, the antennae (Altner and Prillinger 1980; Boeckh et al. 1987; Steinbrecht 1996; Keil 1999). The number of receptor cells per sensillum depends on their function and on species (Rospars 1988). The number of olfactory sensilla per antenna is usually large, for example one antenna of the male moth *Bombyx mori* bears on average 15,000 sensilla trichodea involved in the detection of the sexual pheromone, which contain on average 1.8 ORNs, and 5000 sensilla basiconica containing 4 or 5 ORNs (Schneider and Kaissling 1957; Steinbrecht 1970).

The sensillum complex is embedded in an epithelium with septate (and other) junctions between cells (Keil 1999). This creates an inhomogeneous environment around them and defines an external side, indirectly exposed to air, and an internal side. The dendrites (or cilia) of the neuron are on the external side, surrounded by the sensillum lymph filling the hair lumen (Steinbrecht 1997). Odorant compounds in the air can find their way to them through tiny pores in the hair wall. The rest of the neuron (dendritic trunk, cell body and axon) is on the internal side, partially wrapped by the auxiliary cells. The ionic concentrations of the sensillum lymph and the

J.-P. Rospars (✉)
Unité de Phytopharmacie et Médiateurs Chimiques & Unité de Mathématiques et Informatique Appliquées, Institut National de la Recherche Agronomique, 78026 Cedex Versailles, France
E-mail: rospars@versailles.inra.fr
Tel.: +33-1-30833355
Fax: +33-1-30833119

A. Vermeulen
Royal Netherlands Naval College, Het Nieuwe Diep 8, 1781 AC Den Helder, The Netherlands
E-mail: a.vermeulen@kim.nl

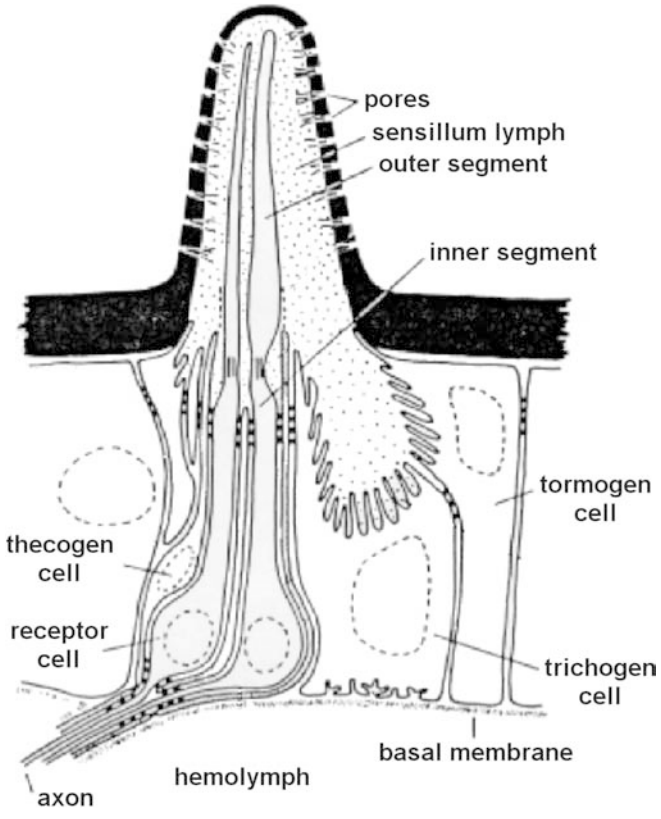

Fig. 1 Schematic representation of the sensillum with two ORNs. The thecogen, tormogen and trichogen cells are auxiliary cells. Adapted from Kaissling (1995)

hemolymph are different and maintained by ionic pumps. They cause a difference of potential between them, across the auxiliary cells: the transepithelial potential, of more than 30 mV (Kaissling and Thorson 1980; Kaissling 1987). The driving force of the receptor potential is thought to be due for a large part to the transepithelial potential (Thurm 1974).

In the present work we consider the generation of the receptor potential in a sensillum with multiple electrically coupled ORNs. Firstly, we summarize a model (Kaissling 1987; Rospars et al. 1996) of the non-electrical part of the transduction process, i.e. the conversion of the odorant concentration to an odorant-dependent conductance increase. This conductance is the input of the electrical model of the sensillum presented in the next sub-sections, which is an extension of our previous single-neuron models (Rospars et al. 1996; Vermeulen and Rospars 1998a, 2001a, 2001b). Secondly, we investigate (in the Results section) the advantages and drawbacks on sensory transduction of the presence of more than one ORN in the sensillum. We do this by considering three different cases of sensillar organization: (1) two or more ORNs with the same sensitivity, (2) two ORNs with different but overlapping sensitivities, and (3) two ORNs with non-overlapping (selective) sensitivities to the same odorant compound. Finally, in the Discussion, we compare our theoretical results to the experimental observations. On this basis we propose an explanation of why case (1) has never been found in nature, and we suggest that case (2) is actually rare.

Model

Model of the biochemical part of the transduction process

The conductance change taking place in the sensory membrane (ORN outer segment) is modelled as the linearly amplified version of the odorant–receptor interaction (Rospars et al. 1996). The membrane is stimulated by an odorant compound A whose concentration is denoted [A] (all symbols used in this subsection are defined in Table 1). The concentration-to-conductance conversion presents two main steps: binding and activation of receptors, then amplification and conductance change. Consider the first step. The membrane bears receptor proteins R of the same type on its surface. The odorant molecules bind to the receptors, then activate them according to the reactions:

$$\mathrm{A} + \mathrm{R} \underset{k_-}{\overset{k_+}{\rightleftarrows}} \mathrm{AR} \underset{k'_-}{\overset{k'_+}{\rightleftarrows}} \mathrm{AR}^* \qquad (1)$$

Table 1 Symbols describing the receptor-to-channel transduction

Parameter	Unit	Description
[A]	M	Concentration of odorant A
$[R_T]$	M	Total concentration of odorant receptor
[R]	M	Concentration of free odorant receptors
[AR]	M	Concentration of receptor–odorant complex
[AR*]	M	Concentration of activated receptor–odorant complex
k_+, k_-	s^{-1} M^{-1}, s^{-1}	Rate constants of the association and dissociation reactions
k'_+, k'_-	s^{-1}	Rate constants of the activation and deactivation reactions
K	M	Equilibrium dissociation constant
K'	–	Equilibrium deactivation constant
κ	–	Ratio of equilibrium dissociation constants for different neurons
r_m	Ω cm	Membrane resistance at rest
g	–	Ratio of the membrane conductance during simulation and at rest
θ	–	Dimensionless conductance g when all receptors are in activated state AR*
g_M	–	g for large [A], $g_M < \theta$
l_S	–	Electrotonic length of the cilia (in membrane space constants)

where k_+, k_-, k'_+ and k'_- are rate constants, AR is the bound receptor–ligand complex and AR* is the activated complex. The concentration of the activated complex at equilibrium is:

$$[\mathrm{AR}^*] = \frac{\frac{[\mathrm{R_T}]}{K'+1}}{1+\frac{KK'}{K'+1}\frac{1}{[\mathrm{A}]}} \tag{2}$$

where $K = k_-/k_+$ and $K' = k'_-/k'_+$ are the equilibrium dissociation and deactivation constants, respectively, and $[\mathrm{R_T}]$ is the total concentration of receptors (ratio of the number of receptors on the membrane to the volume of the sensillum lymph).

In the second step we assume that, through G-protein activation and second messenger production, each activated receptor finally opens Γ odorant-dependent ionic channels with a unit conductance of γ. Hence the (dimensionless) conductance change is given by $g = r_\mathrm{m}\gamma\Gamma[\mathrm{AR}^*]$, using $r_\mathrm{m}{}^{-1}$, the inverse of the membrane resistance at rest r_m, as the unit of conductance. Using Eq. (2) and introducing $\theta = r_\mathrm{m}\gamma\Gamma[\mathrm{R_T}]$, which is the membrane conductance when all receptor-dependent channels are open, the conductance change can be written as:

$$g = \frac{\theta}{1+K'+\frac{KK'}{[\mathrm{A}]}} \tag{3}$$

The maximum value of g when $[\mathrm{A}] \to \infty$ is $g_\mathrm{M} = \theta/(1+K')$. Note that this quantity does not depend on K.

The parameters affecting the odorant-dependent conductance change g are thus θ, K and K'. θ acts as a mere proportionality factor. Increasing K shifts the curve to higher concentrations (Fig. 2), making the neuron less sensitive to the odorant compound, whereas increasing K' mainly decreases the maximum conductance g_M (not shown). In the following, only the effect of K is considered.

Before studying the electrical coupling of neurons with the same or different sensitivities to odorant A, we examine how the conductance change is converted into voltage.

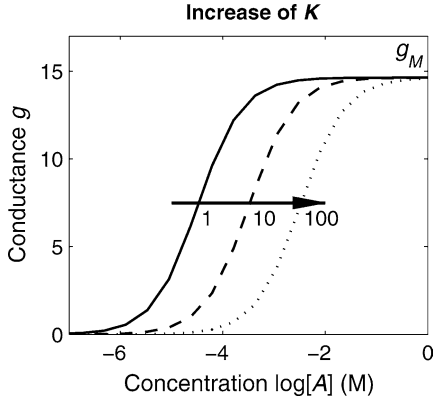

Fig. 2 Influence on conductance of the odorant–receptor equilibrium dissociation constant K controlling the ORN sensitivity to odorant compound A. Decrease in sensitivity due to increase of K, $K = \kappa \times 37.8$ μM with $\kappa = 1$ (*solid line*), 10 (*dashed line*), 100 (*dotted line*). Threshold is defined as the concentrations at which g/g_M is equal to some small value ε, close to zero, and saturation as the concentration at which it is $1-\varepsilon$, close to one. Dynamic range is the distance between threshold and saturation. With $\varepsilon = 5\%$, the threshold of the solid curve is $10^{-5.89}$ M and the dynamic range of all curves is 2.95 decades. Parameters: $K' = 5.8$, $\theta = 100$

Outline of the electrical model

The electrical model of the sensillum is shown in Fig. 3 and the corresponding symbols are defined in Table 2. The sensillum lymph is considered to be isopotential, as well as the hemolymph. Auxiliary cells are modelled with their Thévenin equivalent circuit, i.e. battery E_A in series with resistance R_A (see, for example, Vermeulen and Rospars 1998b). The Thévenin theorem states that any two-terminal circuit can be replaced by the open-circuit voltage source (battery) E in series with resistance R (impedance) obtained when all independent sources are set to zero. No complex resistance (i.e. impedance) has to be considered because we assume the stimulation to be constant and the sensillum to have only linear-time-invariant properties (LTI model).

All ORNs are assumed to have the same morphological and electrical characteristics. The model of the neuron, which is equivalent to the model of Kaissling and Thorson (1980) and to model B of Vermeulen and Rospars (1998a), consists of two circuits connected in series, one corresponding to the sensory dendrite and the other to the non-sensory part of the neuron (dendritic inner segment, soma and axon). Each circuit is replaced by its Thévenin equivalent circuit. The Thévenin equivalent of the sensory dendrite consists of the stimulation-dependent resistance R_TS (which can be different for each neuron and is consequently noted with an additional subscript indicating the neuron number: R_TS1, R_TS2, etc.) and has no batteries. The Thévenin equivalent circuit of the non-sensory part consists of a battery E_rN and a resistance R_in; it is assumed to be the same for

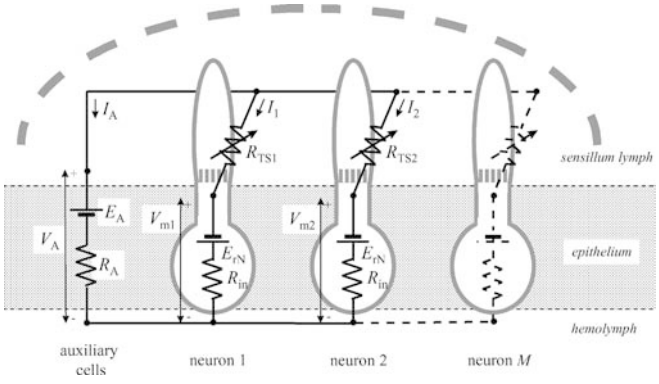

Fig. 3 Electrical model of a sensillum with M ORNs. The sensillum lymph and the hemolymph are each considered isopotential so that the current flows only between them, going through the auxiliary cells and through the neurons. V_A is the transepithelial potential and $V_{\mathrm{m}\,i}$ the transmembrane potential of the non-sensory part of ORN_i. See Table 2 for the electrical components and currents

Table 2 Symbols for the electrical components, currents and potentials (see Fig. 3)

Parameter	Unit	Description
$R_{TS\ i}$	Ω	Thévenin's input resistance of sensory dendrite (outer segment)
R_t	Ω	Input resistance of an unstimulated cylindrical dendrite of infinite length
R_{in}	Ω	Thévenin's input resistance of non-sensory neuron part
R_A	Ω	Resistance simulating auxiliary cells
r_{in}	–	Ratio of R_{in} to R_t
r_A	–	Ratio of R_A to R_t
E_A	V	Battery simulating auxiliary cells
E_{rN}	V	Battery simulating resting potential of non-sensory neuron part
I_A	A	Current flowing through the auxiliary cells
I_i	A	Current flowing through the neuron
V_A	V	Transepithelial potential
V_m	V	Transmembrane potential of non-sensory neuron part
ΔV_A	V	Transepithelial receptor potential
ΔV_m	V	ORN transmembrane receptor potential
V_A^*	–	Transepithelial relative receptor potential
V_m^*	–	ORN transmembrane relative receptor potential
M	–	Number of neurons in the sensillum

all neurons in the sensillum. The resistance R_{TS} is the input resistance of the sensory dendrite as seen from the non-sensory neuron part. It is calculated in Vermeulen and Rospars (1998a, 1998b):

$$R_{TS} = \frac{R_t \coth(\sqrt{1+g}\, l_S)}{\sqrt{1+g}} \tag{4}$$

where l_S is the electrotonic length of the dendrite (expressed in membrane space constants λ), R_t is the input resistance of an unstimulated cylindrical dendrite of infinite length, and g is the dimensionless stimulation-dependent conductance of the neuron considered (see section above on Model of the biochemical part of the transduction process). The calculation of these parameters, knowing the morphological and electrical characteristics of the sensillum, is explained in Vermeulen and Rospars (1998a, 2001a). For a complete numerical example, see Rospars et al. (2003).

Several neurons with the same sensitivity

Consider M identical ORNs with the same sensitivities, i.e. θ, K and K' are the same for all neurons. Consequently, all stimulation-dependent conductances and resistances are the same ($g_1 = g_2 = ... = g$ and $R_{TS1} = R_{TS2} = ... = R_{TS}$) and the same current passes through all neurons ($I_1 = I_2 = ... = I$). The Thévenin equivalent circuit of all ORNs is then given by resistance $(R_{in} + R_{TS})/M$ in series with battery E_{rN}, so the current passing through the auxiliary cells, I_A, is obtained using Ohm's law and Eq. (4):

$$I_A = -\frac{\sum E}{\sum R} = -\frac{E_A + E_{rN}}{R_A + \frac{R_{in}+R_{TS}}{M}} = -\frac{M\sqrt{1+g}(E_A + E_{rN})}{\sqrt{1+g}(MR_A + R_{in}) + R_t \coth(\sqrt{1+g}\, l_S)} \tag{5}$$

The transepithelial potential V_A is given by:

$$V_A = E_A + R_A I_A \tag{6}$$

Substituting Eq. (5) in this formula, we have:

$$V_A = E_A - \frac{MR_A\sqrt{1+g}(E_A + E_{rN})}{\sqrt{1+g}(MR_A + R_{in}) + R_t \coth(\sqrt{1+g}\, l_S)} \tag{7}$$

or, with the use of the dimensionless resistances $r_{in} = R_{in}/R_t$ [this ratio has a different definition in Vermeulen and Rospars (1998a, 2001a, 2001b) where $r_{in} = (R_{in} + R_A)/R_t$] and $r_A = R_A/R_t$:

$$V_A = E_A - \frac{Mr_A\sqrt{1+g}(E_A + E_{rN})}{\sqrt{1+g}(Mr_A + r_{in}) + \coth(\sqrt{1+g}\, l_S)} \tag{8}$$

The membrane potential at the junction of the sensory and non-sensory part of the ORN reflects the potential at the axon initial segment (Rospars et al. 1996; Vermeulen and Rospars 1998b). In the remainder of this work we will call it the transmembrane potential of the non-sensory neuron part. It is the same for all neurons ($V_{m1} = V_{m2} = ... = V_m$) and is given by:

$$V_m = -E_{rN} + R_{in} I \tag{9}$$

The current which flows through the auxiliary cells is equal to the sum of all currents through the ORNs, but of opposite sign: $I_A = -MI$. Thus Eq. (9) becomes, using Eq. (5) and the dimensionless resistances r_{in} and r_A:

$$V_m = -E_{rN} - \frac{R_{in} I_A}{M} = -E_{rN} + \frac{MR_{in}\sqrt{1+g}(E_A + E_{rN})}{\sqrt{1+g}(MR_A + R_{in}) + R_t \coth\left(\sqrt{1+g}\, l_S\right)} = -E_{rN} + \frac{Mr_{in}\sqrt{1+g}(E_A + E_{rN})}{\sqrt{1+g}(Mr_A + r_{in}) + \coth\left(\sqrt{1+g}\, l_S\right)} \tag{10}$$

Two neurons with different sensitivities

We consider now a sensillum containing two identical ORNs, except for the equilibrium dissociation constants

of their receptor proteins with respect to odorant compound A. Let us denote K_1 and K_2 these constants in ORN_1 and ORN_2, respectively, and κ their ratio, $\kappa = K_2/K_1$ with $\kappa \geq 1$. This corresponds to a mere horizontal shift of the ORN_2 conductance versus concentration curve to the right of the ORN_1 curve (see Fig. 2). Thus ORN_2 is less sensitive to A than ORN_1. In the limit, ORN_2 is insensitive to A, which corresponds to $K_2 \to \infty$ and $\kappa \to \infty$. From a modelling point of view, the third sensillum type (one sensitive neuron and the other insensitive) is a special case of the second one (two sensitive neurons with different sensitivities), so Eqs. (11)–(13) apply to both.

The current through the auxiliary cells is now given by:

$$I_A = -\frac{\sum E}{\sum R} = -\frac{E_A + E_{rN}}{R_A + \frac{(R_{in}+R_{TS1})(R_{in}++R_{TS2})}{2R_{in}+R_{TS1}+R_{TS2}}} \quad (11)$$

The transepithelial potential V_A is still given by Eq. (6), but the dendritic membrane potential is now different in each neuron:

$$V_{m1} = -E_{rN} - R_{in}I_1 = -E_{rN} + R_{in}\frac{R_{in}+R_{TS2}}{2R_{in}+R_{TS1}+R_{TS2}}I_A \quad (12)$$

$$V_{m2} = -E_{rN} - R_{in}I_2 = -E_{rN} + R_{in}\frac{R_{in}+R_{TS1}}{2R_{in}+R_{TS1}+R_{TS2}}I_A \quad (13)$$

The derivation of potentials V_A, V_{m1} and V_{m2} as a function of g_1 and g_2 is straightforward. However, the equations are too long to be given here.

Results

Three different types of potential are considered in this section: (1) the difference of potential V between two points taken across the epithelium (transepithelial potential) or across the membrane of the non-sensory part of the ORN (transmembrane potential); (2) the change of transepithelial or transmembrane potential V caused by stimulation g, $\Delta V = V - V_r$, where V_r is the potential at rest, i.e. for $g = 0$; we call it potential change (in the neuron this is the receptor potential stricto sensu), and it can be positive (depolarization) or negative (hyperpolarization); and (3) the normalized receptor potential or relative potential, $V^* = \Delta V/\Delta V_M$, where ΔV_M is the potential change for maximal stimulation as $[A] \to \infty$. Except for θ, numerical values for the model parameters used in the figures (see legend of Fig. 4) are taken or derived from Kaissling (1987, 2001). Selecting $\theta = 100$ gives $g_M \approx 15$, i.e. the maximum conductance change is 15 times the conductance at rest. This value results in the same transepithelial potential for a high odorant concentration, as observed by Kaissling (1987).

Response properties of neurons with the same sensitivity are deteriorated

All three types of transepithelial and neuronal transmembrane potentials are shown in Fig. 4 in the case of a sensillum with M identical ORNs. Although the transepithelial potential, V_A, and the transmembrane potential of the non-sensory part of the ORN, V_m, are different (Fig. 4a and b), the transepithelial potential change ΔV_A is linearly proportional to the receptor potential of the ORNs ΔV_m. The only difference is that their absolute values are different and of opposite sign (Fig. 4c and d). This can also be seen in the relation between the potential changes of the neurons and auxiliary cells derived from Eqs. (8) and (10):

$$\Delta V_m = -\frac{r_{in}}{Mr_A} \times \Delta V_A \quad (14)$$

Consequently, both relative potentials are the same (Fig. 4e and f).

When the number of neurons increases, the relative receptor potentials ($\Delta V_A{}^*$ and $\Delta V_m{}^*$) change only slightly (Fig. 4e and f), but the amplitude of the receptor potentials changes significantly (Figs. 4d and 5a). With the parameter values chosen, the amplitude of the transepithelial receptor potential ΔV_A starts at 24.7 mV for $M = 1$, reaches a maximum of 27.6 mV for $M = 2$, then decreases significantly for more than two ORNs (Fig. 5a, solid line), and that of the transmembrane receptor potential ΔV_m decreases steeply from the same starting point at 24.7 mV (Fig. 5a, dashed line). From a functional point of view, this is a serious disadvantage because the depolarization at the axon initial segment of every neuron also decreases for a given stimulation and a stronger stimulation is necessary to generate the same train of action potentials. Moreover, the absolute threshold linearly increases and the absolute dynamic range linearly decreases with the number of neurons in the sensillum (Fig. 5b and c, dotted lines), although the relative threshold and dynamic range are practically independent of it (solid lines).

Response properties of neurons with different sensitivities are improved

When the sensillum contains two ORNs with different equilibrium dissociation constants ($K_1 \leq K_2$), and consequently different sensitivities to the same compound A, the shape of the concentration–potential curves changes significantly for the three types of potentials considered. This is shown in Fig. 6 for three different values of the ratio $\kappa = K_1/K_2$, with ORN_2 of similar ($\kappa = 10$, left column) and much lower ($\kappa = 10^4$, middle column) sensitivity than ORN_1, and even not sensitive at all (right column).

The change is the easiest to observe for the relative transepithelial and transmembrane potentials (Fig. 6g and h). The transmembrane potential versus

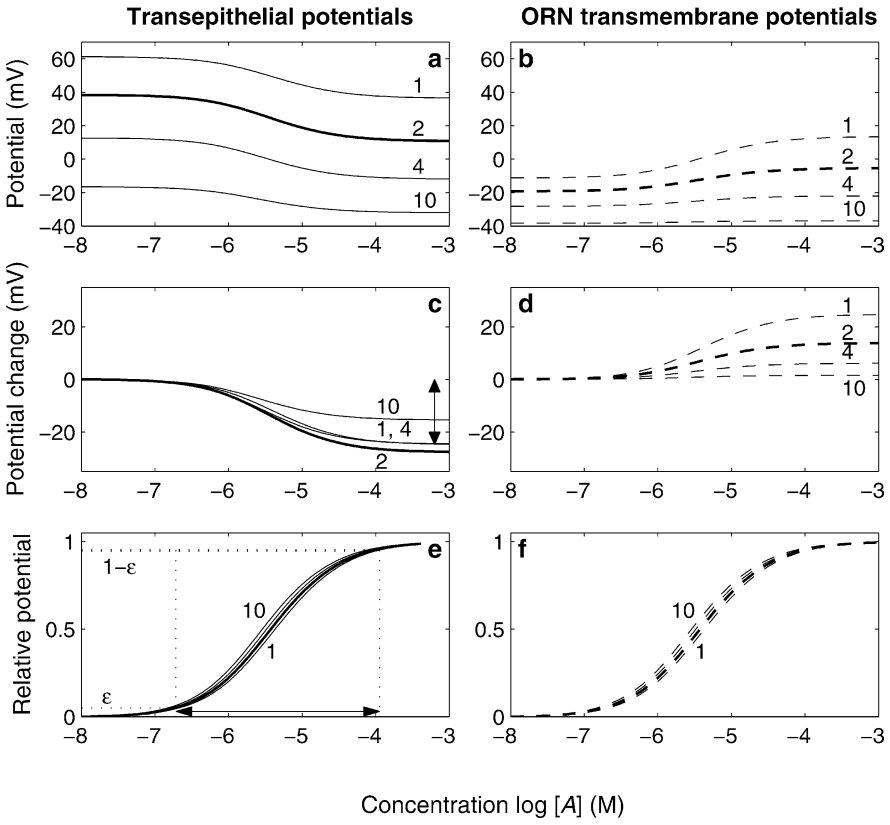

Fig. 4a–f Transepithelial potentials (*left*) and transmembrane potentials of the ORN (*right*) as a function of odorant concentration for a varying number of neurons in the sensillum. All M ORNs are identical with the same sensitivity to the odorant compound and the same morpho-electrical characteristics. *Top row*: transepithelial V_A (Eq. 8) and transmembrane V_m (Eq. 10) potentials. *Middle row*: potential changes ΔV_A and ΔV_m. The *double arrow* in (**c**) indicates the maximum amplitude of the transepithelial potential for $M=1$. *Bottom row*: relative potentials V_A^* and V_m^*. As in Fig. 2, relative threshold (*left vertical dotted line* in **e**) and saturation (*right vertical dotted line* in **e**) are the concentrations at which V_A^* or V_m^* are equal to ε and $1-\varepsilon$, respectively (remember that $0 \le V_A^* \le 1$), and relative dynamic range as the distance between them (*double arrow* in **e**). Parameters: $r_{in}=r_A=0.7$, $l_S=1$, $E_{rN}=50$ mV, $E_A=100$ mV, $\theta=100$, $K=37.8$ μM, $K'=5.8$, $\varepsilon=0.05$, $M=1$, 2 (*thicker lines*), 4, 10, as indicated

concentration curves of the ORNs are no longer of sigmoid shape. The curve of the most sensitive neuron (ORN_1; dashed curve) rises to a maximum (overshoot), then decreases to a constant asymptotic level, whereas the curve of the least sensitive one (ORN_2; dotted curve) decreases to a minimum (undershoot), then increases to the same asymptotic level as the first curve. When the ratio κ, reflecting the difference in sensitivity of the neurons, increases (Fig. 6, middle column), the shape of the curves changes. The threshold moves a little to the left, the maximum and minimum move a little to the right and the point where the curves meet again moves more to the right on the horizontal axis, i.e. towards higher concentrations. As a result, the length of the overshoot or undershoot increases when κ increases. The transepithelial concentration–potential curve is no longer exactly sigmoid (solid curves in Fig. 6). Although it has no overshoot or undershoot, it is "flattened" in the middle. When κ increases, the length of this shoulder increases, the beginning of the shoulder corresponding approximately to the extrema of the transmembrane curves. This shoulder can be easily interpreted as the intermediate zone in the transition from the left part of the curve dominated by the most sensitive neuron, for stimulus concentrations of the order of K_1, to the right part of the curve with the contribution of the least sensitive neuron, for concentrations of the order of κK_1. This qualitative interpretation applies also to a couple of ORNs, one sensitive and the other completely insensitive or only very weakly sensitive to A (i.e. κ is very large). In this case the responses are due to the sensitive ORN alone (Fig. 6, right column). Only the shoulder of the transepithelial potential remains visible in the meaningful range of concentrations and simultaneously the overshoot and undershoot of the transmembrane disappear. In summary, Fig. 6 shows from left to right the complete set of behaviour displayed by the potentials.

Figure 7 illustrates these effects on the response properties (amplitude, threshold and dynamic range). It shows that the amplitude of the transmembrane potential increases with κ, although it remains always smaller than the constant transepithelial potential (Fig. 7a). Both transmembrane and transepithelial thresholds, whether absolute (concentration at which a receptor potential of, for example, 1 mV is reached) or relative (concentration at which a given fraction of the maximum, for example 5%, is reached), are similar and remain practically the same whatever the relative

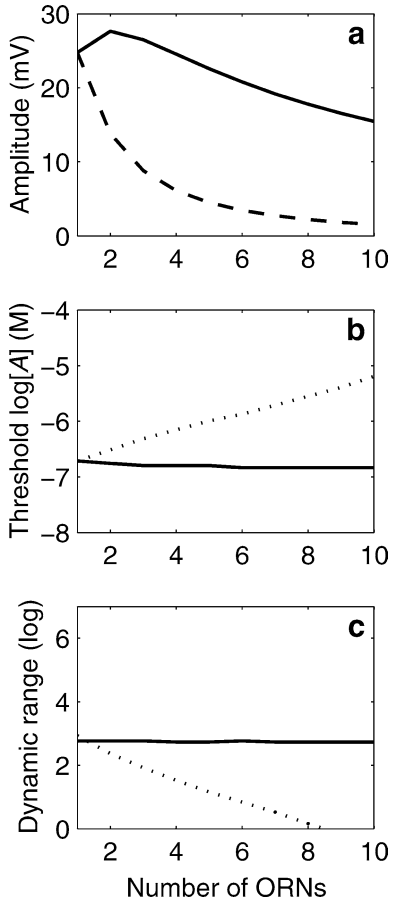

Fig. 5a–c Response properties of transepithelial potential (*solid line*) and ORN transmembrane potential (*dashed line*) as a function of the number of identical ORNs in the sensillum. Relative threshold (**b**, *solid line*) and dynamic range (**c**, *solid line*) defined as in Fig. 4e; transepithelial and transmembrane curves are superimposed. With respect to conductance (see Fig. 2), in the case $M=2$, the relative threshold is lower ($10^{-6.76}$ M = 0.17 μM instead of $10^{-5.89}$ M = 1.29 μM) and the relative dynamic range slightly narrower (2.77 instead of 2.95 decades). Absolute threshold (**b**, *dotted line*) and dynamic range (**c**, *dotted line*) of ORN transmembrane potentials determined on Fig. 4d for $\Delta V_m = 1$ mV (threshold) and $\max(\Delta V_m) - 1$ mV (saturation). Parameters: as in Fig. 4

sensitivities of the ORNs (Fig. 7b). The most remarkable effect is on the dynamic ranges (Fig. 7c). Two dynamic ranges must be distinguished. The first one (overall, solid line) runs from (absolute or relative) threshold to saturation (asymptotic level) and involves the increasing and decreasing parts of the potential; this overall range is equally defined for the transepithelial and transmembrane potentials. The second range (restricted, dashed line) applies only to the ORN_1 transmembrane potential; it goes from threshold to maximum (in fact 1 mV below the maximum for the absolute range or 95% of maximum for the relative range) and so describes the monotonously increasing part of the curve (Fig. 6h). Figure 7c shows that both the overall and restricted ranges increase with the logarithm of κ, although the overall ranges grow linearly while the restricted ranges reach an asymptote. For $\varepsilon = 5\%$ (see definition of ε in Fig. 4) and $K_2 = 22K_1$, the overall relative range is 3.44 and the restricted one is 2.22. When K_2 is 10^6 times greater than K_1, the overall relative range rises to 8.06 and the restricted one reaches 2.93. This effect results entirely from the electrical coupling of the neurons. It cannot occur with an "isolated" neuron (Rospars et al. 1996) or in a single-neuron sensillum, whatever the morphological and electrical characteristics of the neuron (Vermeulen and Rospars 1998a).

Figure 8 shows how the transmembrane receptor potential of the most sensitive ORN in a couple depends on the odorant concentration for various values of κ (Fig. 8a) and of the electrotonic length l_S of the sensory dendrite (Fig. 8b). The latter factor is likely important because of the wide range of variation of dendritic length in different sensilla, from a few micrometres to half a millimetre (see Discussion). Both factors κ and l_S influence the size of the overshoot, which grows with κ up to an asymptotic maximum (Fig. 8c), whereas as a function of l_S it reaches a maximum and then decreases (Fig. 8d).

Discussion

Response characteristics of a sensillum model with several neurons

ORNs in the same sensillum influence each other via passive electrical interaction. For studying this effect, we developed an electrical model of a multi-neuron sensillum. We investigated the influence of the electrical interaction between ORNs on their response properties when they are stimulated by the same odorant compound. The response of the sensillum to a mixture of odorants being still more complex was not considered. This led us to compare three sensillum types according to the response of their ORNs to the odorant, which can be identical, overlapping (one ORN is more sensitive than the other) or selective (only one ORN is sensitive). For these comparisons we utilized the difference of potentials across the auxiliary cells (transepithelial potential) and across the non-sensory dendritic membrane of the ORNs (transmembrane potential). Although the transmembrane potential is the most important to know because it controls the firing rate of the neuron, it cannot be experimentally measured in vivo with the available techniques; it can be only estimated from the firing rate, contrary to the transepithelial potential (see next subsection).

In the single-neuron sensillum, or the sensillum with several identical neurons, the concentration–response curves of the transepithelial potential and of the transmembrane receptor potential of the individual neurons are sigmoid. This is not the case for a pair of neurons with different (overlapping) sensitivities, for which they are no longer sigmoid (Fig. 6).

The transepithelial curve presents a shoulder in the middle whose length depends on the ratio κ of the

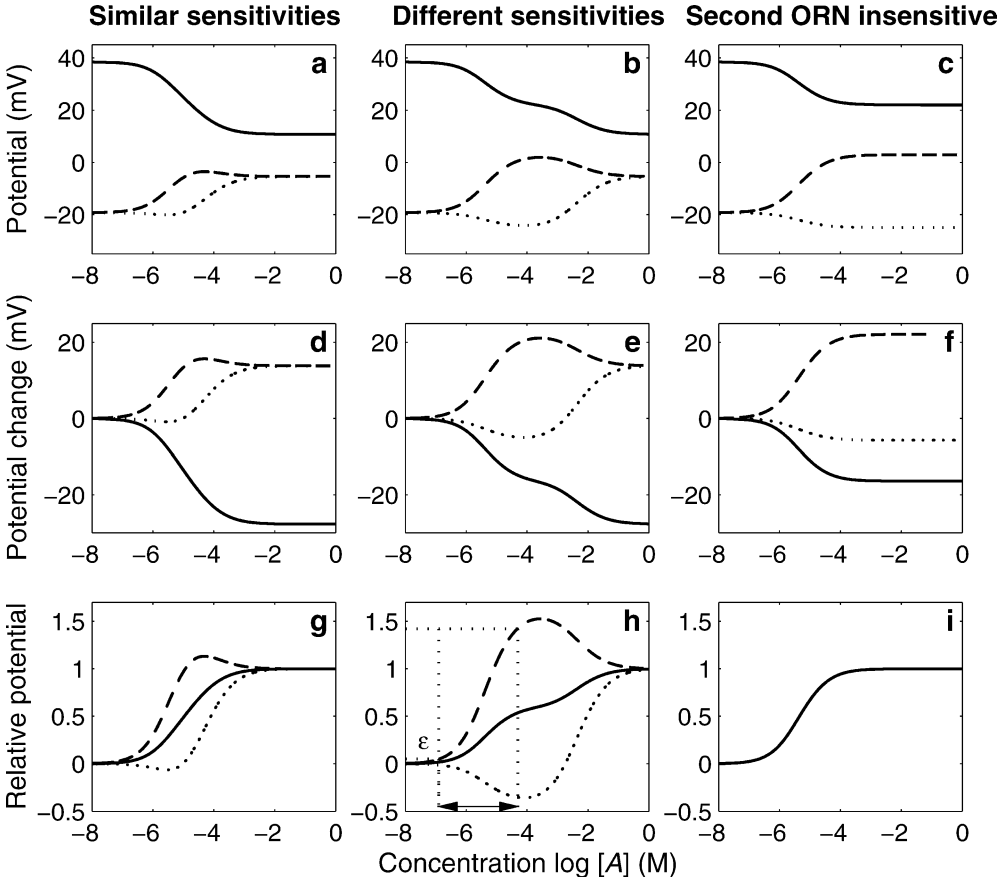

Fig. 6a–i Comparison of dose–response curves for a pair of ORNs with ORN_1 very sensitive to an odorant and ORN_2 slightly less sensitive ($\kappa = 10$, *left column*), much less sensitive ($\kappa = 10^4$, *middle column*) and not sensitive at all ($\kappa \to \infty$, *right column*) to the same odorant. The ORNs differ only by their sensitivities, i.e. the ratio of the equilibrium dissociation constants, $\kappa = K_2/K_1$. *Top row*: transepithelial potential V_A (*solid line*) and transmembrane potentials for ORN_1 V_{m1} (*dashed line*) and ORN_2 V_{m2} (*dotted line*) are shown. *Middle row*: potential changes ΔV_A (*solid line*), ΔV_{m1} (*dashed line*) and ΔV_{m2} (*dotted line*). *Bottom row*: relative potentials V_A^* (*solid line*), V_{m1}^* (*dashed line*) and V_{m2}^* (*dotted line*). In (**h**) the restricted dynamic range is indicated [end point is taken at $(1-\varepsilon)\max(V_m^*)$; compare with Fig. 4e]. Parameters: as in Fig. 4, except $M = 1$, $K_1 = K$, $K_2 = \kappa K_1$

equilibrium dissociation constants characterizing the neurons. When κ increases, the shoulder moves to the right on the concentration axis. It results in the increase of the dynamic range of the transepithelial receptor potential, which is the most significant effect of co-localizing neurons with different but overlapping sensitivities. In contrast, neither the threshold nor the amplitude of the transepithelial potential are much modified, except in the limit case of a completely insensitive second neuron, for which the amplitude is reduced.

The transmembrane potential of the least sensitive neuron presents an undershoot and that of the most sensitive neuron an overshoot. When κ increases, the overshoot and the undershoot move to the right on the concentration axis (compare second and third columns of Fig. 6) so that, in the limit case of a completely insensitive second neuron ($\kappa \to \infty$), the curves become sigmoid again. Then the insensitive neuron responds to the stimulation with a hyperpolarization and can be considered, from a modelling point of view, as an auxiliary cell, so this special case is equivalent to that of the sensillum model with a single ORN surrounded by auxiliary cells studied in a previous work (Vermeulen and Rospars 1998a). The varieties of shape of the transmembrane receptor potential versus concentration curves have several consequences on the response properties of the ORNs, which can be summarized as follows.

1. Gathering in the same sensillum several ORNs with the same biochemical, electrical and morphological characteristics has no apparent advantages and at least one serious drawback, because the transmembrane receptor potential at the axon initial segment is decreased for all ORNs, with a corresponding increase of the absolute threshold and narrowing of the absolute dynamic range. The larger the number of identical ORNs per sensillum, the greater the decrease.
2. Co-localization in the same sensillum of two ORNs sensitive to the same compound, but with different sensitivities, presents some advantages. Starting from two identical neurons and then increasing the ratio κ of the equilibrium dissociation constants of the neurons, i.e. putting together neurons more and more dissimilar, increases the amplitude of the transmembrane receptor potential of the most sensitive neuron and slightly lowers its threshold. If only the monotonous part of the concentration–response curve is considered, no improvement of the dynamic range is obtained. The presence of an overshoot, however, poses a potential problem for coding odour intensity, since the same receptor potential, and consequently the same firing rate, can encode two different stimulus intensities.
3. Gathering in the same sensillum two ORNs, one sensitive to the odorant compound and the other completely insensitive to it, maximally increases the

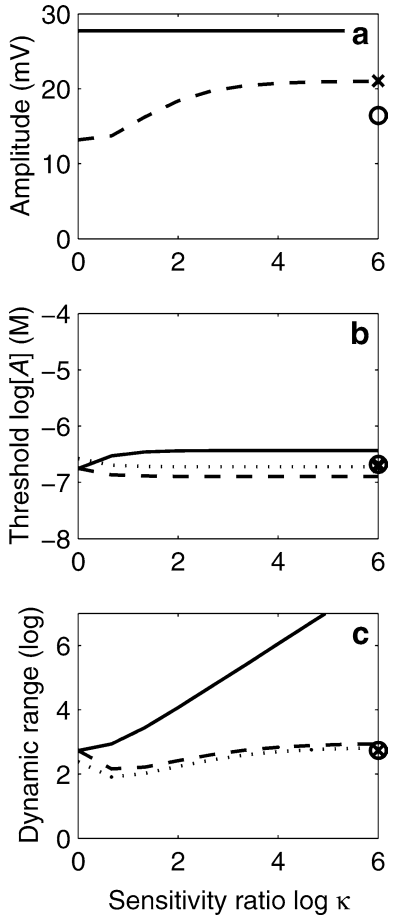

Fig. 7a–c Response properties of transepithelial potential (*solid line*) and ORN_1 transmembrane potential (*dashed* and *dotted lines*) for the pair of neurons shown in Fig. 6. These ORNs differ only by their sensitivities to odorant A, i.e. the ratio of the equilibrium dissociation constants, $\kappa = K_2/K_1$. Transepithelial (*circle*) and transmembrane (*cross*) potentials for very large κ, i.e. ORN_2 insensitive to odorant A, are shown on the *right*. In (**b**) are the relative threshold of the transepithelial potential (*solid line*), relative (*dashed line*) and absolute (*dotted line*, see legend of Fig. 5) thresholds of the transmembrane receptor potential; the corresponding points for very large κ (on *right margin*) are practically superimposed. In (**c**) are the same representations for the dynamic ranges: full relative range for the transepithelial potential (from threshold to asymptotic saturation, see *arrow* in Fig. 4e); restricted dynamic ranges of the transmembrane potential of ORN_1 (monotonously increasing part of the curve only, see *arrow* in Fig. 6h for the relative range, and corresponding part of the dashed curve in Fig. 6e for the absolute range). Parameters: as in Fig. 6

amplitude of the transmembrane receptor potential of the sensitive neuron. It gives an intermediate threshold and intermediate dynamic range with respect to pairs of identical neurons, on the one hand, and to pairs of neurons with different sensitivities, on the other hand.

Comparison with experimental data

The transepithelial potential and the action potentials can be recorded by cutting the extremity of the hair and slipping a pipette on it (Kaissling 1995). A theoretical analysis of this system shows that the tip-recorded potential is an excellent approximation of the transepithelial potential (Vermeulen and Rospars 2001a). Another commonly used technique for recording action potentials consists in inserting a tungsten wire electrode into the base of the sensillum (Boeckh et al. 1987). The transmembrane potentials cannot be measured directly with these extracellular techniques. However, they are reflected in the firing rates of the ORNs. In sensilla with only two (active) ORNs, individual rates can be determined from the different sizes of the action potentials of both cells, even when they are identical (Meunier et al. 2003).

Insect olfactory sensilla have been thoroughly investigated, especially the trichoid sensilla of moths (Zack 1979; Kaissling and Thorson 1980; Kaissling 1987). These long sensilla house two ORNs, each sensitive to one of the two components of the sexual pheromone, e.g. bombykol and bombykal in *Bombyx mori*. The transepithelial potential and the firing frequency were measured using the tip-recording technique and both were found to be sigmoid in shape as a function of concentration. The ratio κ of the dissociation reaction constants of the pheromone components for the bombykol ORN, for example, is not known, although it can be considered as large. This is consistent with the shape of the curves of the transepithelial potential for $\kappa = 10^4$, shown in Fig. 6e (the shoulder of the experimental curve, being small, might be hidden in the experimental variability), and that of the transmembrane potential in Fig. 8a (curve c); or, if $\kappa > 10^4$, with the shapes shown in Figs. 6f and 8a (curve d), respectively.

Concentration–response curves were determined also for small sensilla housing ORNs sensitive to food odours, e.g. in the cockroach *Periplaneta americana* (Selzer 1984). The sensilla sensitive to food odours are more diverse than those sensitive to pheromones. For this reason, a sensillum housing ORNs with well-defined olfactory spectra is more difficult to identify and repeatedly investigate, which makes the assessment of the respective sensitivities of ORNs in the same sensillum difficult. A significant advance in this direction, however, was the recent identification of physiological types of neurons and sensilla in *Drosophila melanogaster*, permitting repeated measurements of the firing rate of a given ORN type (de Bruyne et al. 1999, 2001). All complete dose–response curves established by these authors are sigmoid in shape. Qualitatively, the 2– 4 ORNs in a same sensillum are usually sensitive to different series of compounds, although in one sensillum type (ab1), two of the neurons, although different, responded strongly to ethyl acetate (de Bruyne et al. 2001). In this case also the dose–response curve of one neuron was found sigmoid. That of the other was not determined, so that κ is not known, although likely small (corresponding to left column of Fig. 6).

Therefore, the sensilla investigated so far give no evidence for the pairing of identical ORNs in the same

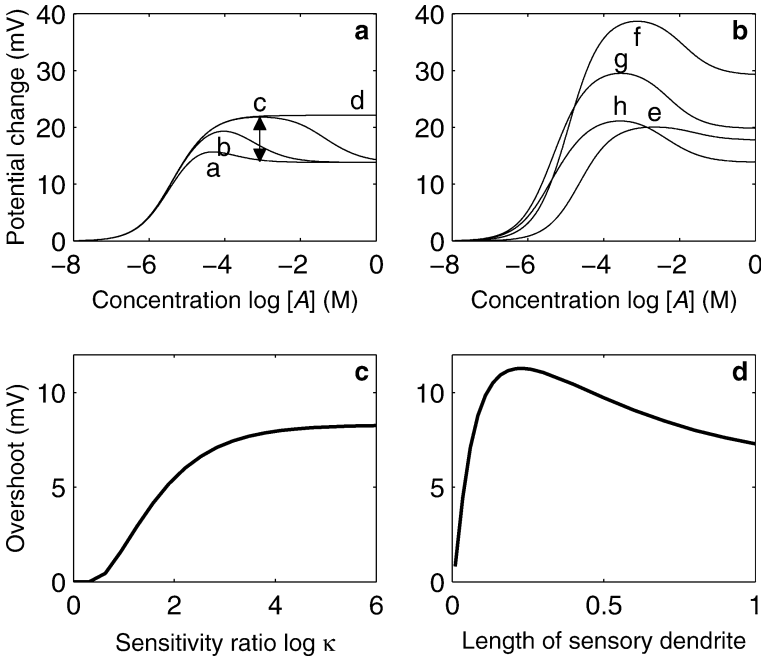

Fig. 8a–d Transmembrane receptor potential of most sensitive ORN (*top row*) and size of the overshoot, i.e. difference between maximum and asymptotic values of the receptor potential (*bottom row*). (**a**) Transmembrane receptor potential for various values of the sensitivity ratio $\kappa = 10$ (*a*), 100 (*b*), 10^4 (*c*), ∞ (*d*), for dendritic length $l_S = 1$ membrane space constant. The *double arrow* indicates the size of the overshoot for curve *c*. (**b**) Transmembrane receptor potential for various values of electronic length l_S of the sensory dendrite: 0.02 (*e*), 0.1 (*f*), 0.5 (*g*), 1 (*h*), for $\kappa = 10^3$. (**c**) Size of the overshoot as a function of κ. (**d**) Size of the overshoot as a function of l_S. Parameters: as in Fig. 6, except l_S

sensillum (reviewed in Todd and Baker 1999). This can be interpreted in the framework of the present model, which shows that gathering two (or more) identical ORNs would decrease the amplitude of the transmembrane potential. The two remaining possibilities, namely pairing of ORNs with either overlapping or selective sensitivities, can, in principle, be distinguished by the sigmoid (selective ORNs) or non-sigmoid (overlapping ORNs) shape of the dose–response curves. The fact that only sigmoid shapes have been observed, as yet, may signify that ORNs with overlapping sensitivities are actually rare.

However, the available evidence is inconclusive because, to our knowledge, no complete dose–response curves to the same odorant of both neurons in a sensillum have been established yet. Further investigations on a larger sample of identified sensilla and odorants are needed to assess the rarity of non-sigmoid curves. Moreover, the presence of a shoulder in the transepithelial potential and of an overshoot in the transmembrane potential might be difficult to observe for other reasons. (1) For a pheromone-sensitive ORN, these effects might not be visible because the sensitivity to the pheromone components are very different (large κ). This is consistent with the equality of the dynamic ranges for the transepithelial receptor potential and the firing rate in moth pheromone ORNs (Zack 1979). (2) For an ORN responding to many odorants with overlapping sensitivities (food odours), the effects might not be seen because the dendrites are too short (see Fig. 8). (3) In the studied model, the maximum conductances in both neurons are assumed equal, whatever their sensitivities (see Fig. 2). If the stimulus with the highest threshold evokes a smaller maximal conductance, the effects produced, including the size of the overshoot, will be smaller than in the present model. (4) The model applies to the transmembrane potential, which was never measured in vivo, and is only indirectly related to the firing rate. If the firing rate is not a linear function of the transmembrane receptor potential, the observation of an overshoot of the latter may be prevented. This is the case, for example, when the maximum rate is reached before saturation of the receptor potential. (5) In the electrical model studied the ORNs contain no "active" components. This seems justified for the ORNs housed in the trichoid sensilla of moths (for references see above), but might be wrong for other sensilla. Interpretations (2) to (5) may apply to the response to ethyl acetate of the ab1 sensillum type mentioned above (de Bruyne et al. 2001). Choosing between these alternatives calls for further experimental and computational studies.

Other reasons for grouping ORNs into sensilla

The presence in sensilla of pairs or triplets of ORNs with different sensitivities may have other reasons than the electrical interaction between them in the same sensillum. Developmental and other physiological reasons are also important, and their inventory is likely far from being completed. For example, such grouping permits, by a series of controlled cell divisions during development (Keil 1999), obtention of the same numbers of ORNs of two or three different types on the antenna. Moreover, recent experiments by Fadamiro et al. (1999) showed that the *Heliothis zea* males can discriminate whether a single or two pheromone components are present in the same filament of the pheromone plume. According to the authors, this is possible only if the pair of different ORNs involved in the reception of these components are co-compartmentalized within the same sensillum (see discussion in Todd and Baker 1999).

Acknowledgements We thank Prof. Karl-Ernst Kaissling, Prof. Frédéric Marion-Poll and Dr Philippe Lucas for useful comments on a previous version of this manuscript.

References

Altner H, Prillinger L (1980) Ultrastructure of invertebrate chemo-, thermo-, and hygroreceptors and its functional significance. Int Rev Cytol 67:69–139

Boeckh J, Ernst KD, Selsam P (1987) Neurophysiology and neuroanatomy of the olfactory pathway in the cockroach. In: Roper SD, Atema J (eds) Olfaction and taste IX. New York Academy of Sciences, New York, pp 39–43

Buck LB (1996) Information coding in the vertebrate olfactory system. Annu Rev Neurosci 19:517–544

de Bruyne M, Clyne PJ, Carlson JR (1999) Odor coding in a model olfactory organ: the *Drosophila* maxillary palp. J Neurosci 19:4520–4532

de Bruyne M, Foster K, Carlson JR (2001) Odor coding in the *Drosophila* antenna. Neuron 30:537–552

Fadamiro HY, Cosse AA, Baker TC (1999) Fine-scale resolution of closely spaced pheromone and antagonist filaments by flying male *Helicoverpa zea*. J Comp Physiol A 185:131–141

Hildebrand JG, Shepherd GM (1997) Mechanisms of olfactory discrimination: converging evidence for common principles across phyla. Annu Rev Neurosci 20:595–631

Kaissling K-E (1987) In Colbow K (ed) RH Wright lectures on insect olfaction. Simon Fraser University, Burnaby, BC, Canada

Kaissling K-E (1995) Single unit and electroantennogram recordings in insect olfactory organs. In: Spielman AI, Brand JG (eds) Experimental cell biology of taste and olfaction, current techniques and protocols. CRC Press, Boca Raton, pp 361–377

Kaissling K-E (2001) Olfactory perireceptor and receptor events in moths: a kinetic model. Chem Senses 26:125–150

Kaissling K-E, Thorson J (1980) Insect olfactory sensilla: structural, chemical and electrical aspects of the functional organization. In: Satelle DB, Hall LM, Hildebrand JG (eds) Receptors for neurotransmitters, hormones and pheromones in insects. Elsevier, Amsterdam, pp 261–282

Keil TA (1999) Morphology and development of the peripheral olfactory organs. In: Hansson B (ed) Insect olfaction. Springer, Berlin Heidelberg New York, pp 5–47

Krieger J, Breer H (1999) Olfactory reception in invertebrates. Science 286:720–723

Meunier N, Marion-Poll F, Rospars JP, Tanimura T (2003) Coding of bitter taste in *Drosophila*. J Neurobiol 56:139–152

Rospars J-P (1988) Structure and development of the insect antennodeutocerebral system. Int J Insect Morphol Embryol 17:243–294

Rospars J-P, Lansky P, Tuckwell H, Vermeulen A (1996) Coding of odor intensity in a steady-state deterministic model of an olfactory receptor neuron. J Comput Neurosci 3:51–72

Rospars J-P, Lansky P, Duchamp-Viret P, Duchamp A (2003) Relation between stimulus and response in frog olfactory receptor neurons *in vivo*. Eur J Neurosci 18:1135–1154

Schneider D, Kaissling KE (1957) Der Bau der Antenne des Seidenspinners *Bombyx mori* L. II. Sensillen, cuticulare Bildungen und innerer Bau. Zool Jahrb Abt Anat Ontog Tiere 76:223–250

Selzer R (1984) On the specificities of antennal olfactory receptor cells of *Periplaneta americana*. Chem Senses 8:375–395

Steinbrecht RA (1970) Zur Morphometrie der Antenne des Seidenspinners, *Bombyx mori* L.: Zahl und Verteilung des Riechsensillen (Insecta, Lepidoptera). Z Morphol Tiere 68:93–126

Steinbrecht RA (1996) Structure and function of insect olfactory sensilla. In: Bock GR, Cardew G (eds) Olfaction in mosquito-host interactions. Wiley, Chichester, pp 158–177

Steinbrecht RA (1997) Pore structures in insect olfactory sensilla: a review of data and concept. Int J Insect Morphol Embryol 26:229–245

Thurm U (1974) Basics of the generation of receptor potentials in epidermal mechanoreceptors of insects. In: Schwartzkopff J (ed) Symposium on mechanoreception. Rheinisch-Westfälische Akademie der Wissenschaften, Abhandlung Band 53. Westdeutscher Verlag, pp 355–385

Todd JL, Baker TC (1999) Function of peripheral olfactory organs. In: Hansson B (ed) Insect olfaction. Springer, Berlin Heidelberg New York, pp 67–96

Vermeulen A, Rospars J-P (1998a) Dendritic integration in olfactory sensory neurons: a steady-state analysis of how the neuron structure and neuron environment influence the coding of odor intensity. J Comput Neurosci 5:243–266

Vermeulen A, Rospars J-P (1998b) A simple analytical method for determining the steady-state potential in models of geometrically complex neurons. J Neurosci Methods 82:123–133

Vermeulen A, Rospars J-P (2001a) Membrane potential and its electrode-recorded counterpart in an electrical model of an olfactory sensillum. Eur Biophys J 29:587–596

Vermeulen A, Rospars J-P (2001b) Electrical circuitry of an insect olfactory sensillum. Neurocomputing 32–40:1011–1017

Zack C (1979) Sensory adaptation in the sex pheromone receptor cells of saturniid moths. Doctoral thesis, LMU München, pp 1–99